$DyBe_{13}$ magnetic structure: neutron diffraction and Mossbauer study

1985 J. Phys. F: Met. Phys. 15 181

(http://iopscience.iop.org/0305-4608/15/1/020)

J. Phys. F: Met. Phys. **15** (1985) 181–192. Printed in Great Britain

$DyBe_{13}$ magnetic structure: neutron diffraction and Mössbauer study

F Vigneron†, M Bonnet‡ and J Chappert§

† Laboratoire Léon Brillouin, CEN-Saclay, F-91191 Gif sur Yvette Cedex, France
‡ Institut Laue–Langevin, 156X Centre de Tri, F-38042 Grenoble Cedex, France
§ Departement de Recherche Fondamentale, CEN-Grenoble 85X, F-38041 Grenoble Cedex, France

Received 26 April 1984, in final form 20 July 1984

Abstract. A neutron diffraction study ($\lambda = 1.140$ Å) of the cubic intermetallic compound $DyBe_{13}$ has shown that below $T_N = 10 \pm 0.5$ K $DyBe_{13}$ exhibits a commensurate magnetic structure with a propagation vector $\boldsymbol{\tau} = \frac{1}{3}\boldsymbol{c}^*$ and magnetic moments of the Dy^{3+} ions ($\boldsymbol{M}_1$, $\boldsymbol{M}_2$ and $\boldsymbol{M}_3$ with $M_2 = M_3$) perpendicular to the crystallographic $\boldsymbol{c}$ axis. As powder neutron diffraction data can only yield two relations between M_1, $M_2 = M_3$ and $\varphi = (\boldsymbol{M}_1, \boldsymbol{M}_2)$, identical Dy^{3+} magnetic moments were assumed ($M = M_1 = M_2 = M_3$). A Mössbauer effect investigation of the same compound is reported in the temperature range 1.5–15 K. Below the magnetic ordering temperature $T_N = 10$ K the results are interpreted within a model including either two magnetic sites ($M_1 \neq M_2 = M_3$, $T = 1.5$ K) or one site ($M_1 = M_2 = M_3$) and relaxation. A self-consistent analysis of the magnetic structure, with a Hamiltonian including exchange and crystalline electric field components, shows that M_1 and M_2 are neither identical nor significantly different ($\Delta M/M \leqslant 1\%$).

1. Introduction

Neutron diffraction experiments on rare-earth beryllides $REBe_{13}$ (Fm3c cubic space group) have been reported for RE = Tb (Vigneron *et al* 1980) and RE = Gd (Vigneron *et al* 1982). The magnetic structure observed depends on the rare earth. $GdBe_{13}$ exhibits a helimagnetic structure below $T_N = 27 \pm 2$ K, with a propagation vector $\boldsymbol{\tau} = 0.285\boldsymbol{c}^*$ independent of temperature and Gd^{3+} magnetic moments perpendicular to the crystallographic $\boldsymbol{c}$ axis.

The situation is more complex for $TbBe_{13}$ due to the competition between exchange interactions and anisotropy ($GdBe_{13}$ is a compound with negligible magnetocrystalline anisotropy). The Tb^{3+} magnetic moments are always perpendicular to the $\boldsymbol{c}$ axis; their relative arrangement can be regarded as a regular (in the temperature range between 11 K and $T_N = 16.5 \pm 0.5$ K) or distorted (below 11 K) helical structure. The propagation vector $\boldsymbol{\tau}$ of the magnetic structure varies with the temperature of the sample: $\boldsymbol{\tau}$ is equal to $\frac{1}{3}\boldsymbol{c}^*$ below $T_{N'} = 8.5$ K and to $\frac{1}{3}(1 - \varepsilon(T))\boldsymbol{c}^*$ in the temperature range $T_{N'} - T_N$.

$DyBe_{13}$ is another example of a compound with competing exchange interaction and anisotropy. Magnetic measurements on this compound indicate a magnetic ordering temperature of 9 K (Bucher *et al* 1975) or 9.3 K (Herr *et al* 1975) and a positive Curie paramagnetic temperature $\theta_p = 13$ K (Herr *et al* 1975).

The results reported here have been obtained from neutron diffraction and Mössbauer effect studies of a polycrystalline sample of $DyBe_{13}$. This sample has been prepared by

high-frequency induction melting in a BeO crucible, in a pure argon atmosphere, starting with 99.9% pure Dy and Be.

2. $DyBe_{13}$: neutron diffraction study

Neutron diffraction patterns have been obtained at Saclay for $\lambda = 1.140$ Å in the paramagnetic region ($T = 300$ K) and below T_N ($T = 4.2$ K). Due to the large absorption cross section of natural Dy for thermal neutrons ($\sigma_a \simeq 600$ b at $\lambda \simeq 1$ Å) the measurements were carried out in the symmetrical transmission geometry (in a sample holder of 2.5×7.5 mm^2 section). The experimental determination of the linear absorption coefficient of the $DyBe_{13}$ polycrystalline sample yields $\mu = 3.7$ cm^{-1}. As the neutron counts at a Bragg position 2θ are proportional to $A(\theta) = lt \exp(-\mu t/\cos\theta)$ where lt is the volume of the sample in the incident beam, and $A(0)$ is maximum for $\mu t = 1$, we have chosen $t = 2.5$ mm for the thickness of the sample holder ($\mu t \simeq 1$). For a maximum value of 44° for 2θ, the ratio $(A(\theta) - A(0))/A(0)$ of the absorption factors does not exceed 10^{-2}. No absorption correction was then used.

2.1. Crystalline structure ($T = 300$ K)

$DyBe_{13}$ crystallises in the cubic $NaZn_{13}$-type structure (space group Fm3c) with eight Dy in $\frac{1}{4}\,\frac{1}{4}\,\frac{1}{4}$, eight Be_I in 0 0 0 and 96 Be_{II} in 0 y z. A refinement of the nuclear pattern (see table 1) with scattering lengths $b_{Dy} = 1.69 \times 10^{-12}$ cm and $b_{Be} = 0.774 \times 10^{-12}$ cm (Bacon 1972) leads to $a = 10.210(2)$ Å, $y = 0.1150(4)$, $z = 0.1775(5)$ and the isotropic Debye parameter $B = 0.5(1)$ Å^2, with a reliability factor $R = \Sigma|I_{obs} - I_{calc}|/\Sigma I_{obs} = 1.6\%$.

2.2. Magnetic structure at $T = 4.2$ K

The neutron diffraction pattern of $DyBe_{13}$ at 4.2 K is shown in figure 1 in the 2θ range 4°–27°. The nuclear Bragg peaks 200_N, 220_N, 222_N and 400_N are indicated in the (a, a, a) cubic cell. Magnetic Bragg peaks have appeared which can be indexed in a (a, a, $3a$) magnetic cell, with h and k even and l odd. This kind of magnetic pattern has already been observed for the isomorphous compound $TbBe_{13}$ below $T_{N'} = 8.5$ K (Vigneron *et al* 1980).

Table 1. $DyBe_{13}$ nuclear Bragg peaks at $T = 300$ K. The observed intensities, I_{obs}, with their estimated errors in brackets, and the calculated intensities, I_{calc}, with $I_{calc} = \frac{1}{2}(j\langle F_K^2\rangle/\sin\theta \sin 2\theta)\exp(-2B\sin^2\theta/\lambda^2)$ are given. F_K is the nuclear structure factor for $\boldsymbol{K} = h\boldsymbol{a}^* + k\boldsymbol{b}^* + l\boldsymbol{c}^*$.

hkl	I_{obs}	I_{calc} (b/nuclear cell)
200	3478(454)	3474
220	4635(370)	3941
222	8776(340)	9073
400	5857(326)	6140
420	44651(424)	43751
422	80111(498)	79471
531	124661(728)	124591
{600 442	19013(513)	20740

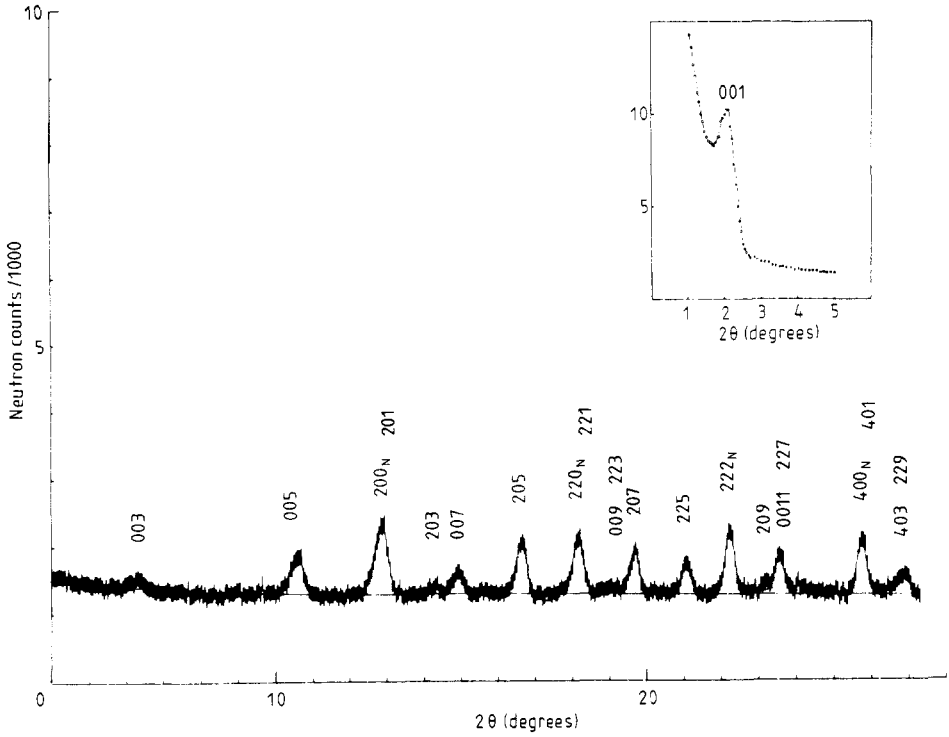

Figure 1. Profile refinement for $DyBe_{13}$ magnetic structure with $T = 4.2$ K and $\lambda = 1.14$ Å. Nuclear hkl_N Bragg peaks are indexed in the (a, a, a) cubic cell and magnetic hkl Bragg peaks in the commensurate $(a, a, 3a)$ magnetic cell.

The magnetic structure is then described by a succession of ferromagnetic (001) planes, with the RE^{3+} magnetic moments arranged in the sequence $\boldsymbol{M}_1$, $\boldsymbol{M}_2$, $\boldsymbol{M}_3$, $-\boldsymbol{M}_1$, $-\boldsymbol{M}_2$, $-\boldsymbol{M}_3$ (cf figure 2).

From a powder neutron diffraction experiment on $REBe_{13}$, only four quantities can be obtained (Vigneron *et al* 1980): $\Sigma_{i=1}^{3} M_i^2$, $\Sigma_{i=1}^{3} (M_i^z)^2$, $(\boldsymbol{M}_1 - \boldsymbol{M}_2 + \boldsymbol{M}_3)^2$ and $(M_1^z - M_2^z + M_3^z)^2$, where M_i^z stands for the component of $\boldsymbol{M}_i$ parallel to the $\boldsymbol{c}$ axis.

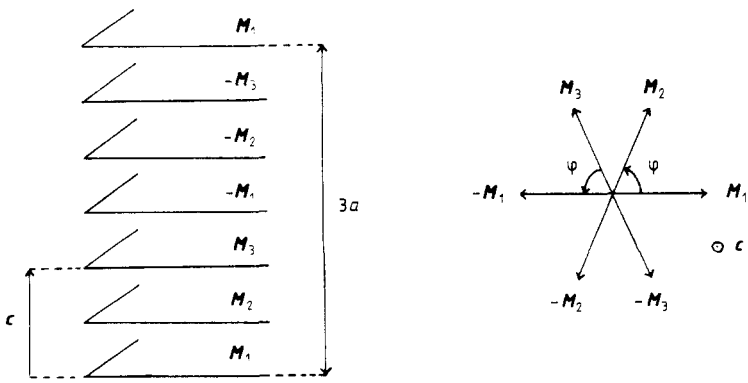

Figure 2. Commensurate $(a, a, 3a)$ magnetic structure of $DyBe_{13}$. The Dy^{3+} ions form a simple cubic arrangement of parameter $a/2$.

An intensity analysis of the magnetic lines for $TbBe_{13}$ and $DyBe_{13}$ shows that the magnetic moments $\boldsymbol{M}_i$ are perpendicular to the $\boldsymbol{c}$ axis. A minimisation of the anisotropy energy (see Vigneron *et al* 1980) shows that $\boldsymbol{M}_1$, $\boldsymbol{M}_2$ and $\boldsymbol{M}_3$ are arranged in the configuration shown in figure 2: $\boldsymbol{M}_1$ is parallel to an easy magnetisation axis in a (001) plane and $\boldsymbol{M}_2$ and $\boldsymbol{M}_3$ are symmetric relative to the perpendicular easy axis in the plane. The commensurate $(a, a, 3a)$ $REBe_{13}$ magnetic structure is then defined entirely by the three parameters M_1, $M_2 = M_3$ and $\varphi = (\boldsymbol{M}_1, \boldsymbol{M}_2)$. As the powder neutron diffraction data can only yield two quantities, $\Sigma_{i=1}^{3} M_i^2$ and $(M_1 - 2M_2 \cos\varphi)^2$, equal Dy^{3+} moments were assumed.

With this assumption $(M_1 = M_2 = M_3 = M)$ the profile refinement (Rietveld 1969) of the neutron diffraction pattern at $T = 4.2$ K gives $M = (8.5 \pm 0.1)\,\mu_B$ and $\varphi = (\boldsymbol{M}_1, \boldsymbol{M}_2) = (80 \pm 2)°$.

For this analysis, no Debye parameter is considered (since $\sin\theta/\lambda < 0.2$ Å^{-1}) and the magnetic form factor for Dy^{3+} is calculated in the spherical dipolar approximation from the results of Freeman and Desclaux (1979).

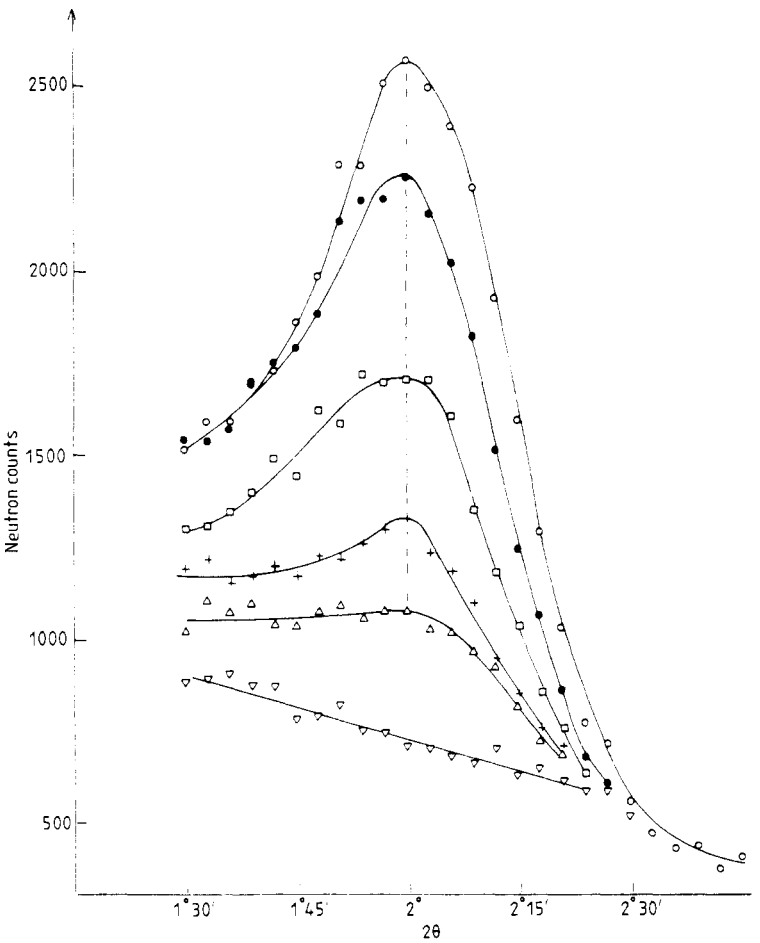

Figure 3. Thermal variation of the magnetic structure of $DyBe_{13}$. The curves are for temperatures of: ○, 4.2 K; ●, 6 K; □, 8 K; +, 9 K; △, 9.5 K; ▽, 11 K. The position of the 001 magnetic Bragg peak is independent of T.

2.3. Thermal variation of the magnetic structure

Figures 3 and 4 show the thermal variation of the 001 magnetic Bragg peak of $DyBe_{13}$. It can be seen (figure 3) that its position does not change with T, unlike $TbBe_{13}$ in which the propagation vector τ of the magnetic structure does not remain equal to $\frac{1}{3}c^*$ up to the Néel temperature $T_N = 16.5$ K. From the variation of its intensity as a function of T (figure 4), the magnetic ordering temperature of $DyBe_{13}$ is found to be $T_N = (10 \pm 0.5)$ K. So a commensurate $(a, a, 3a)$ magnetic structure is observed for $DyBe_{13}$ at any temperature below T_N. This structure is defined by the values of the three magnetic moments, $\boldsymbol{M}_1$, $\boldsymbol{M}_2$ and $\boldsymbol{M}_3$ (cf figure 2), corresponding to the three parameters M_1, $M_2 = M_3$ and $\varphi = (\boldsymbol{M}_1, \boldsymbol{M}_2)$. In order to check the single-moment assumption $(M = M_1 = M_2 = M_3)$ a Mössbauer experiment has been performed, which is described below.

3. $DyBe_{13}$: a Mössbauer study

3.1. Experimental conditions

Mössbauer absorption spectra have been obtained for $DyBe_{13}$ (Grenoble, DRF/LIH) in the temperature range 1.5–15 K using a spectrometer in the sinusoidal mode. The sample was prepared by mixing an appropriate weight of $DyBe_{13}$ powder with Araldite.

The Mössbauer resonance is $E_\gamma = 25.65$ keV for the ^{161}Dy nucleus (of natural isotopic abundance 19%). This line corresponds to an E1 transition between the ground $I_g = \frac{5}{2}^+$ and the excited $I_e = \frac{5}{2}^-$ nuclear levels (figure 5).

A single line source was obtained from ^{161}Tb. This was obtained by neutron irradiation of 20 mg of 90% enriched $^{160}GdF_3$, with an irradiation time of 7 days and a neutron flux of 1.5×10^{14} neutrons cm^{-2} s^{-1}. The source lifetime is about 7 days.

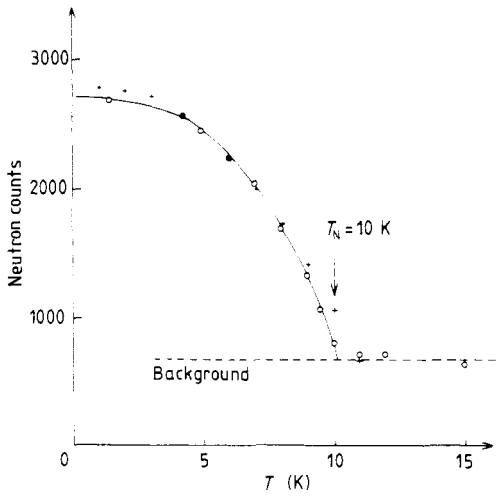

Figure 4. Determination of the Néel temperature T_N of $DyBe_{13}$. The points show the experimental (O) and calculated (+) neutron counts at $2\theta = 2°$. The calculated values are obtained using the self-consistent model described in § 4.

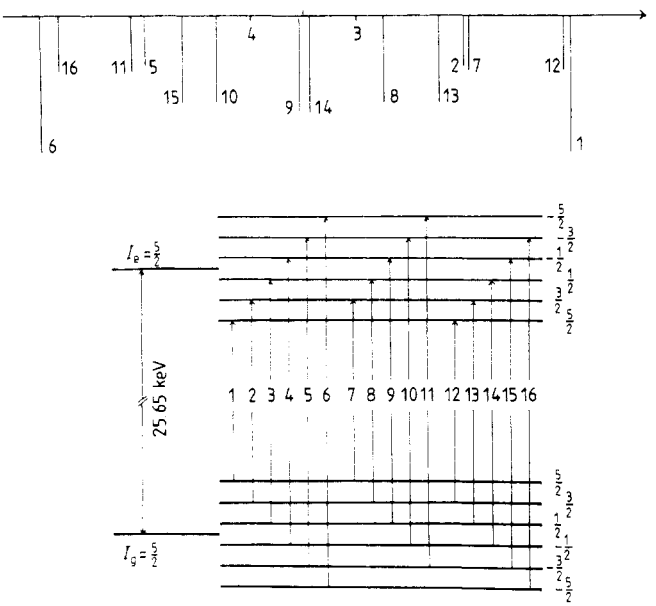

Figure 5. Nuclear E1 transitions of ^{161}Dy. On the level scheme the splitting of each I manifold is only due to a Zeeman Hamiltonian $-g_N \mu_N H_{eff} I_z$, for the sake of simplicity. However, the position of the Mössbauer lines in the upper diagram (which has a linear energy scale) also takes into account a quadrupolar Hamiltonian $\mathscr{H}_Q$.

3.2. $DyBe_{13}$: Mössbauer absorption spectrum at $T = 1.5$ K

The Mössbauer spectrum at 1.5 K is shown in figure 6; it has been analysed taking into account one or two sets of Hamiltonians $\mathscr{H} = \mathscr{H}_Z + \mathscr{H}_Q$. $\mathscr{H}_Z$ is the nuclear Zeeman Hamiltonian $-g_N \mu_N \boldsymbol{I} \cdot \boldsymbol{H}_{eff} = -g_N \mu_N I_z H_{eff}$ where z is a local axis parallel to the electronic magnetic moment $\boldsymbol{M}_i$ of the Dy^{3+} ion. The effective magnetic field at the Dy nucleus, H_{eff}, is proportional to M_i within the fast-relaxation assumption. $\mathscr{H}_Q$ is the quadrupolar Hamiltonian $\frac{1}{4}e^2qQ[3I_z^2 - I(I+1)]/I(2I-1)$ where Q is the nuclear quadrupolar moment and q is the magnetically induced electric field gradient for $T < T_N$. (No electric field gradient exists in the paramagnetic region, due to the cubic symmetry of the rare-earth crystalline site.)

By assuming identical Dy^{3+} magnetic moments ($M_1 = M_2 = M_3$), only one value of H_{eff}, and consequently of e^2qQ, is to be considered. A least-squares fit of the experimental Mössbauer pattern leads to $H_{eff} = 5308(2)$ kOe, $e^2qQ = 115.6(3)$ mm s^{-1}, the isomer shift $\delta = 1.40(4)$ mm s^{-1} and the full width at half maximum for a Lorentzian curve of $\Gamma = 9.65(15)$ mm s^{-1}.

Assuming two different values for the Dy^{3+} magnetic moments (M_1 and $M_2 = M_3$), two values of H_{eff} and of e^2qQ are necessary for the spectrum analysis. Then the least-squares fit of the experimental Mössbauer pattern leads to $H_{eff}(1) = 5249(5)$ kOe, $(e^2qQ)(1) = 112.5(5)$ mm s^{-1} and $I(1) = 0.535(15)$ for one value, and $H_{eff}(2) = 5377(3)$ kOe, $(e^2qQ)(2) = 120.5(5)$ mm s^{-1} and $I(2) = 0.465(15)$ for the other value, both with $\delta = 1.35(4)$ mm s^{-1} and $\Gamma = 7.20(10)$ mm s^{-1}.

Let us notice here the relative weight ($I(1)/I(2) \simeq 1$) of the two superposed spectra. This result does not reproduce the experimental neutron diffraction situation $I(1)/I(2) = \frac{1}{2}$. But

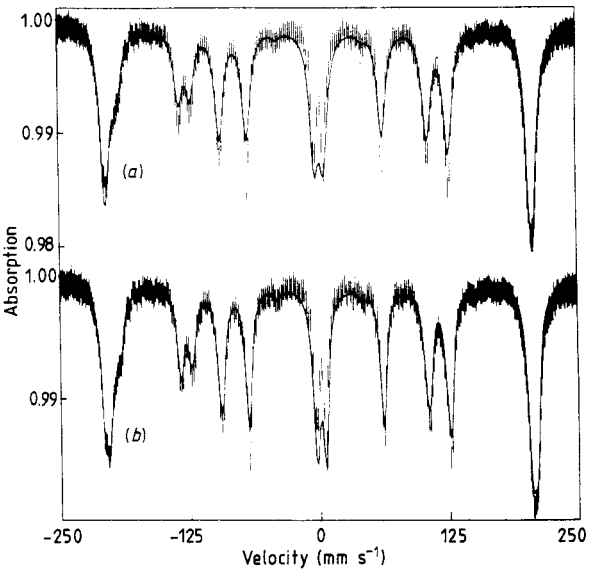

Figure 6. Mössbauer absorption spectrum of $DyBe_{13}$ at $T = 1.5$ K. The vertical lines indicate the experimental counts and their accuracies, defined by counts $\pm 2\sqrt{\text{counts}}$. The full curve corresponds to a static model of superposition of (*a*) one or (*b*) two Mössbauer spectra ($\mathscr{H} = \mathscr{H}_Z + \mathscr{H}_Q$).

the least-squares fit obtained with this last constraint is not very different from the case $I(1)/I(2) = 1$, as χ^2 takes the value 2.95 instead of 2.75. As a matter of comparison, χ^2 is equal to 3.95 with only one value of H_{eff} and of e^2qQ (figure 6(*a*)).

As $H_{\text{eff}}(i)$ is proportional to M_i (J is a good quantum number) we can deduce from the previous results a mean value over the different magnetic sites for the Dy^{3+} electronic magnetic moment at $T = 1.5$ K of $M = 9.35\,\mu_B$ and its relative variation, also over the different magnetic sites, of $\Delta M/M = 2.5\%$.

3.3. $DyBe_{13}$: Mössbauer absorption spectra above and below T_N

Several Mössbauer spectra have been obtained for $DyBe_{13}$ at $T \geqslant 1.5$ K (figures 7 and 8). Up to 9.9 K the spectra show the typical 16 lines of magnetically ordered $DyBe_{13}$, and at $T \geqslant 10$ K there is a unique peak at $V = 0$ (except for the isomer shift). The magnetic ordering temperature of $DyBe_{13}$, measured in the Mössbauer experiment, is then identical to that measured in the neutron diffraction experiment and is $T_N = 10$ K.

All these spectra have been analysed taking into account the relaxation effects between the two sublevels of the ground electronic doublet of Dy^{3+}. For the analysis, identical electronic magnetic moments are assumed for Dy^{3+} ($M_1 = M_2 = M_3$). The model of Nowik and Wickman (1966) has been used below T_N (ferromagnetic relaxation) and that of Dattagupta (1981) above T_N (paramagnetic relaxation).

At very low temperatures only the ground sublevel of the electronic doublet is populated, so no relaxation effects are expected. The Mössbauer pattern is then only determined by the four parameters defined in § 3.2: H_0 (effective magnetic field), e^2qQ, δ (isomer shift) and Γ (Lorentzian width). From $H_0 = 5308$ kOe ($T = 1.5$ K $\ll T_N$) and

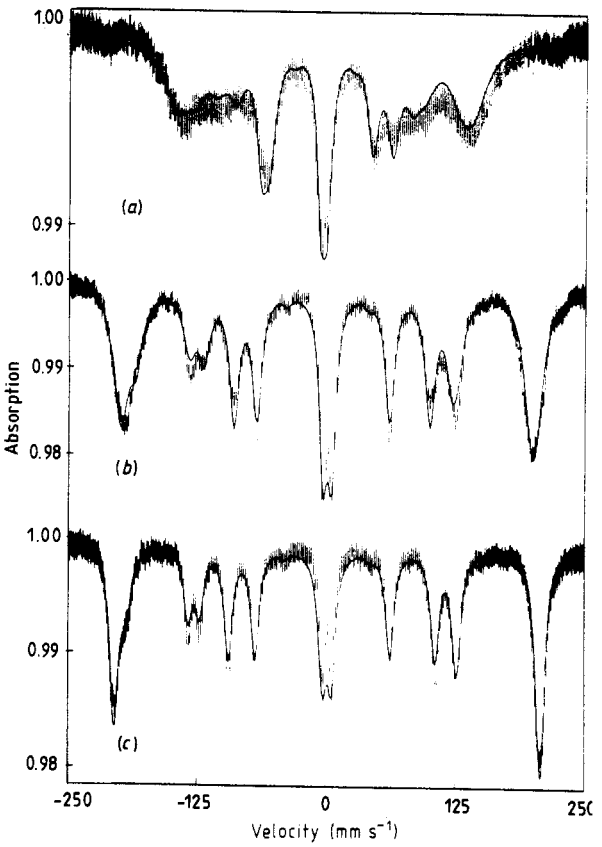

Figure 7. Mössbauer absorption spectra of $DyBe_{13}$ at $T < T_N$ for (*a*) 8 K, (*b*) 4 K and (*c*) 1.5 K. The full curves assume the relaxation model of Nowik and Wickman (1966). The vertical lines are as in figure 6.

$\frac{1}{2}A_{\parallel}I_z = g_N\mu_N H_0 I_z$ we can easily obtain $A_{\parallel} = 73.95$ mm s^{-1} for the hyperfine constant of the ^{161}Dy nuclear level.

In the present analysis we have taken $A_{\parallel} = 73.95$ mm s^{-1} and $A_{\perp} = 0$ below T_N, and $A_{\parallel} = A_{\perp} = 73.95$ mm s^{-1} above T_N. The values of δ and Γ are also kept constant and equal to 1.40 mm s^{-1} and 9.65 mm s^{-1}, respectively.

Table 2. Relaxation parameters as a function of temperature for the $DyBe_{13}$ Mössbauer study. Two models of relaxation have been used, the model of Nowik and Wickman (1966) at $T < T_N$ and that of Dattagupta (1981) at $T \geqslant T_N$.

T(K)	e^2qQ (mm s^{-1})	$W = \hbar/\tau$ (mm s^{-1})	Δ(K)
4	101.6 ± 0.8	625 ± 120	15.5 ± 0.5
6	78.5 ± 1.0	1250 ± 85	17 ± 0.5
8	45.5 ± 1.5	2030 ± 95	13.5 ± 0.5
10	0	1600 ± 100	0
10.5	0	1775 ± 100	0
15	0	8450 ± 300	0
300	0	13400 ± 950	0

Below T_N the parameters of the model are then e^2qQ, Δ (the Zeeman splitting between the two sublevels of the ground electronic doublet of Dy^{3+}) and τ or W (where τ is the relaxation time and $W=\hbar/\tau$). Above T_N both e^2qQ and Δ are zero, since there is cubic symmetry and no induced quadrupole effect.

The results are given in table 2 and represented in figures 7, 8 and 9. For $W=1500\ \text{mm s}^{-1}$ (the mean value for $T\leqslant 10.5$ K), τ is equal to 0.5×10^{-11} s. This relaxation time is characteristic of a spin–spin mechanism.

Let us note that the asymmetry of the Mössbauer line observed in the temperature range above T_N (figure 8) can be accounted for (Henning *et al* 1970) by a dispersion effect, which has not, however, been considered in our analysis.

4. Discussion and conclusions

The neutron diffraction and Mössbauer experiments have given the same value for the magnetic ordering temperature of $DyBe_{13}$, $T_N=(10\pm0.5)$ K, a result which is consistent with the values obtained from susceptibility measurements (Bucher *et al* 1975, Herr *et al* 1975).

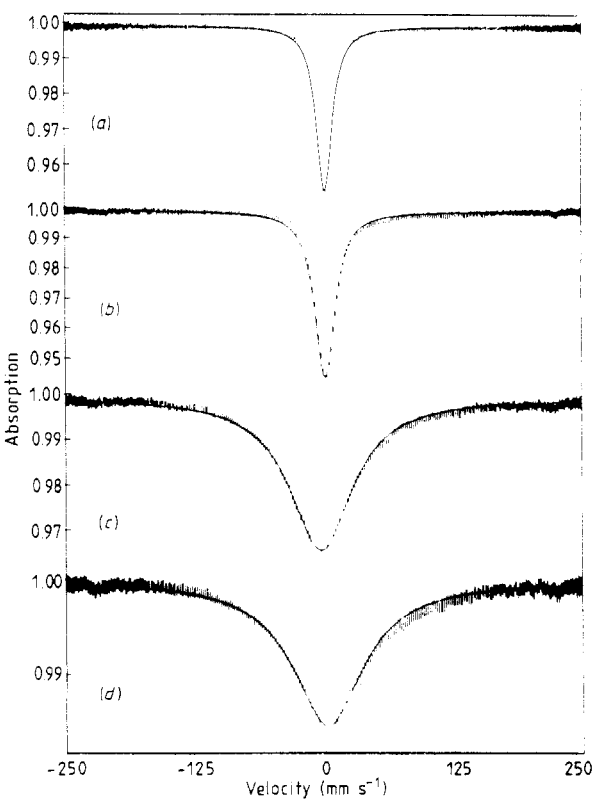

Figure 8. Mössbauer absorption spectra of $DyBe_{13}$ at $T\geqslant T_N$ for (*a*) 300 K, (*b*) 15 K, (*c*) 10.5 K and (*d*) 10 K. The full curves assume the relaxation model of Dattagupta (1981). The vertical lines are as in figure 6.

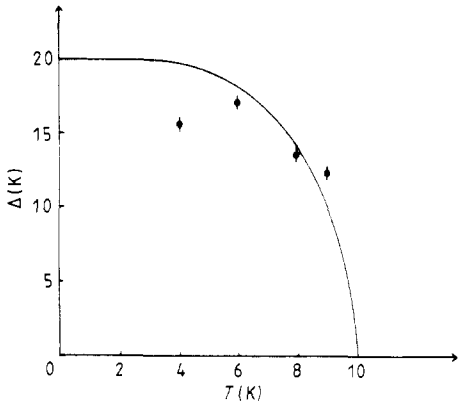

Figure 9. Mössbauer study of $DyBe_{13}$ below T_N, showing the splitting of the electronic ground state (doublet) as a function of temperature. The full curve corresponds to a molecular field model $\Delta = 2k_B T_N \tanh(\Delta/2k_B T_N)$ with $T_N = 10$ K.

The values obtained for the Dy^{3+} magnetic moment at $T = 1.5$ K are $(8.75 \pm 0.50)\,\mu_B$ and $9.35\,\mu_B$, the neutron diffraction result from the thermal variation of the 001 magnetic Bragg peak (see figure 4) and the Mössbauer result, respectively; they are in reasonable agreement with each other.

The magnetic structure of $DyBe_{13}$ has been found to be different from that of other rare-earth–Be_{13} intermetallic compounds (with RE = Gd, Tb) in that the magnetic unit cell (a, a, $3a$) is commensurate with the crystalline cubic cell (a, a, a) at any temperature below T_N. This property results from the growing influence of the crystalline anisotropy from gadolinium (Gd^{3+} is an S state, $L = 0$) to terbium ($L = 3$) and dysprosium ($L = 5$).

In the description of the $DyBe_{13}$ magnetic structure, identical Dy^{3+} magnetic moments were assumed, giving $M = M_1 = M_2 (= M_3)$. The analysis of the Mössbauer spectrum at 1.5 K has given some indication for $M_1 \neq M_2$, but with no significantly different values ($\Delta M/M = 2.5\%$). So this result is not inconsistent with the single-moment assumption which was necessary for the powder neutron diffraction analysis. For the Mössbauer analysis in the temperature range from 1.5 K to T_N, identical Dy^{3+} magnetic moments have been assumed in order to limit the number of the refined parameters. In this analysis, using the relaxation model of Nowik and Wickman (1966), the electronic ground state of any Dy^{3+} ion is a doublet with magnetic moments $\pm 9.35\,\mu_B$.

The electronic level scheme of Dy^{3+} can be obtained from the diagonalisation of the Hamiltonian $\mathcal{H} = \mathcal{H}_{CEF} + \mathcal{H}_{EXCH}$ within the $J = \frac{15}{2}$ manifold. $\mathcal{H}_{CEF}$ is the crystalline electric field Hamiltonian. For cubic symmetry (at the rare-earth site in $DyBe_{13}$) it can be written (Lea *et al* 1962) as

$$\mathcal{H}_{CEF} = W\left(x\frac{O_4}{F(4)} + (1-|x|)\frac{O_6}{F(6)}\right)$$

where O_4 and O_6 are the Stevens equivalent operators, $F(4)$ and $F(6)$ are numerical constants (for $J = \frac{15}{2}$, $F(4) = 60$ and $F(6) = 13\,860$) and W and $-1 \leqslant x \leqslant +1$ are the CEF parameters. $\mathcal{H}_{EXCH}$ is the exchange Hamiltonian. In a molecular field model, for a rare earth labelled i ($i = 1, 2, 3$; see figure 2), we can write

$$\mathcal{H}_{EXCH}(i) = -g_J \mu_B \boldsymbol{J}_i \cdot \boldsymbol{H}_m(i)$$

Table 3. $DyBe_{13}$ magnetic structure from a self-consistent calculation with $W=0.0425$ K, $x=-0.045$, $J_0=3950$ Oe μ_B^{-1} and $J_1-J_2=500$ Oe μ_B^{-1}.

T(K)	$M_1(\mu_B)$	$M_2(\mu_B)$	$\varphi=(M_1, M_2)$(degrees)
1	9.220	9.300	84.35
2	9.200	9.275	84.10
3	9.050	9.120	82.65
4.2	8.640	8.675	78.55
6	7.750	7.685	68.90
7	7.120	7.055	64.65
8	6.340	6.300	62.25
9	5.320	5.305	60.95
10	3.875	3.870	60.30

with

$$\boldsymbol{H}_m(1)=J_0\boldsymbol{M}_1+(J_1-J_2)(\boldsymbol{M}_2-\boldsymbol{M}_3)$$

$$\boldsymbol{H}_m(2)=J_0\boldsymbol{M}_2+(J_1-J_2)(\boldsymbol{M}_1+\boldsymbol{M}_3)$$

$$\boldsymbol{H}_m(3)=J_0\boldsymbol{M}_3+(J_1-J_2)(-\boldsymbol{M}_1+\boldsymbol{M}_2).$$

The exchange parameters J_0, J_1 and J_2 characterise the interactions between a magnetic moment $\boldsymbol{M}_i=g_J\mu_B\langle\boldsymbol{J}_i\rangle$ and all its neighbours in the same $\{J_0\}$, nearest-neighbour $\{J_1\}$ and next-nearest-neighbour $\{J_2\}$ (001) rare-earth planes. $\langle\boldsymbol{J}_i\rangle$ is the mean value of the kinetic moment calculated in the Maxwell–Boltzmann statistics.

The CEF parameters W and x have been determined from specific-heat measurements on $LaBe_{13}$, $PrBe_{13}$ and $TmBe_{13}$ compounds (Bucher *et al* 1975). A linear interpolation from the results for praseodymium and thulium leads to $W=0.0425$ K and $x=-0.045$ for $DyBe_{13}$. These values give an overall CEF splitting of 24 K, a CEF ground state Γ_7 ($\pm\frac{34}{9}\mu_B$) and a $\Gamma_8^{(1)}$ first-excited level (where $\Gamma_7-\Gamma_8^{(1)}=6$ K), in good agreement with the EPR results on **La**$DyBe_{13}$ of Bloch *et al* (1978) and Dokter *et al* (1978).

From the neutron diffraction data at $T=4.2$ K of $\Sigma_{i=1}^{3}\boldsymbol{M}_i^2=223(5)\mu_B^2$ and $(\boldsymbol{M}_1-\boldsymbol{M}_2+\boldsymbol{M}_3)^2=28(5)\mu_B^2$, a least-squares method was used to determine the exchange parameters J_0 and J_1-J_2. The best fit between the experimental data and the self-consistently calculated magnetic structure leads to $J_0=3950$ Oe μ_B^{-1} and $J_1-J_2=500$ Oe μ_B^{-1}.

The self-consistent values of M_1, M_2 and $\varphi=(\boldsymbol{M}_1, \boldsymbol{M}_2)$ for $W=0.0425$ K, $x=-0.045$, $J_0=3950$ Oe μ_B^{-1} and $J_1-J_2=500$ Oe μ_B^{-1} are listed in table 3. The corresponding intensity calculated for the 001 magnetic Bragg peak is shown in figure 4; the theoretical magnetic ordering temperature is then equal to 11 K, while experimentally $T_N=(10\pm0.5)$ K.

We must note that, for the self-consistent results in table 3, M_1 and M_2 are nearly identical: the maximum value of the ratio $\Delta M/M$ is equal to 1%.

Acknowledgments

The authors would like to thank A Herr of the University of Strasbourg for the preparation of the $DyBe_{13}$ sample and M Bogé of CEN-Grenoble for his assistance in the Mössbauer

experiment. They would also like to thank P Bonville and J Hodges of CEN-Saclay for helpful discussions on the influence of relaxation on the Mössbauer absorption spectra. They are grateful to P Meriel of CEN-Saclay for his assistance in the neutron diffraction experiment and a careful reading of the manuscript.

References

Bacon G E 1972 *Acta Crystallogr.* A **28** 357
Bloch J M, Davidov D, Dokter H D, Felner I and Shaltiel D 1978 *J. Phys. F: Met. Phys.* **8** 1805
Bucher E, Maita J P, Hull G W, Fulton R C and Cooper A S 1975 *Phys. Rev.* B **11** 440
Dattagupta S 1981 *Hyperfine Interactions* **11** 1977
Dokter H D, Davidov D, Bloch J M, Felner I and Shaltiel D 1978 *J. Magn. Magn. Mater.* **7** 78
Freeman A J and Desclaux J P 1979 *J. Magn. Magn. Mater.* **12** 11
Henning W, Baehre G and Kienle P 1970 *Phys. Lett.* **31B** 203
Herr A, Besnus M J and Meyer A 1975 *Coll. Int. CNRS, Physique sous Champs Magnétiques Intenses* p 47
Lea K R, Leask M J M and Wolf W P 1962 *J. Phys. Chem. Solids* **23** 1381
Nowik I and Wickman H H 1966 *Phys. Rev. Lett.* **17** 949
Rietveld H M 1969 *J. Appl. Crystallogr.* **2** 65
Vigneron F, Bonnet M, Herr A and Schweizer J 1982 *J. Phys. F: Met. Phys.* **12** 223
Vigneron F, Sougi M, Meriel P, Herr A and Meyer A 1980 *J. Physique* **41** 123